Supporting Information for

Investigating major sources of methane emissions at US landfills

by

Tia R. Scarpelli[1]*, Daniel H. Cusworth[1], Riley M. Duren[1], Jinsol Kim[1], Joseph Heckler[2], Gregory P. Asner[2], Eben Thoma[3], Max J. Krause[3], Daniel Heins[3], Susan Thorneloe[3]

[1]Carbon Mapper, Pasadena, CA, 91101, USA
[2]Center for Global Discovery and Conservation Science, Arizona State University, Tempe, AZ, 85287, USA
[3]US Environmental Protection Agency, Washington, DC, 20004, USA
*Corresponding author: tia@carbonmapper.org

This document contains 9 Pages and 8 Figures and is accompanied by an .xlsx file (Landfill Data 2023.xlsx).

Radiant Heat Detection Methodology

The Global Airborne Observatory (GAO) spectrometer can be used to identify active destruction devices like flares, as described by Cusworth et al.[1]. Thresholding is applied to the nonmethane radiance channels (1945-2485 nm), separating background reflected solar radiance from radiance emitted from active destruction devices. We apply this thresholding to the entire scene, and we compare the location of the known control stacks at the landfill, identified using visible imagery, with the locations of detected heat signals from destruction devices.

References

(1) Cusworth, D.H., Duren, R., Thorpe, A., Olson-Duvall, W., Heckler, J., Chapman, J., Eastwood, M., Helmlinger, M.C., Green, R. O., Asner, G.P., Dennison, P.E., Miller, C.E.: Intermittency of large methane emitters in the Permian Basin, Environ. Sci. Technol. Lett., 8, 567–73, https://doi.org/10.1021/acs.estlett.1c00173, 2021.

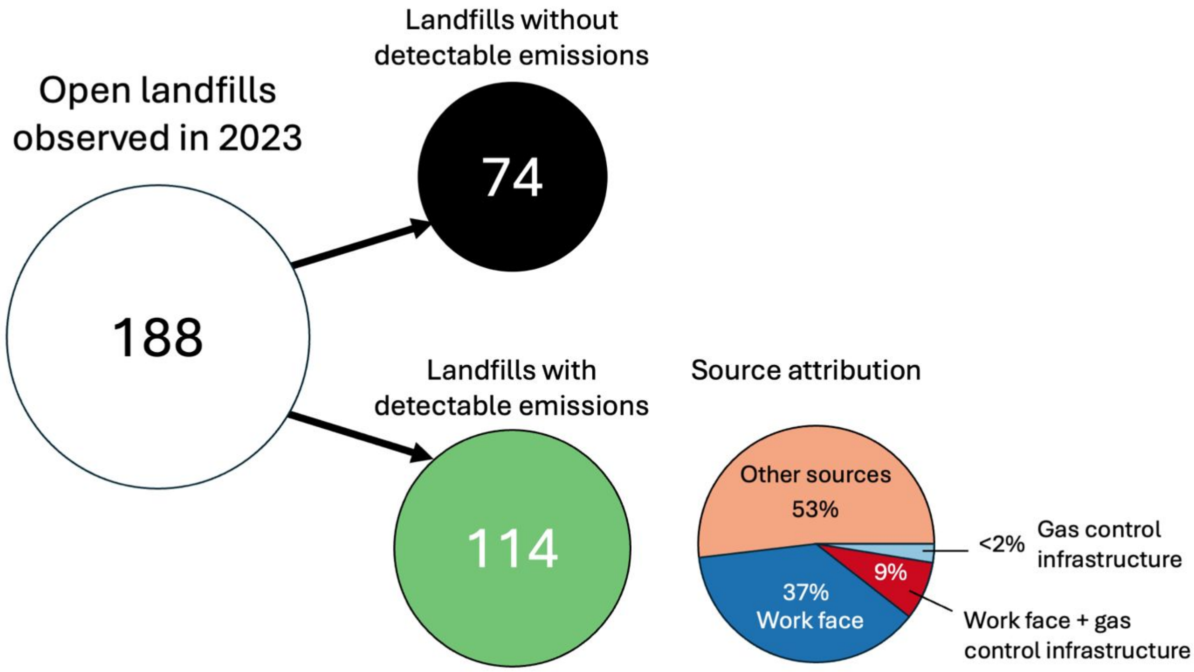

Figure S1. Diagram showing the total number of open landfills observed by category. We only show open landfills to align with Figure 3. Of the open landfills observed, we show the breakdown between those with (green) and without (black) detectable emissions (i.e., detectable point source emissions). For landfills with detectable emissions, we also show the percentage of emitting landfills for each source attribution category as defined in Figure 3.

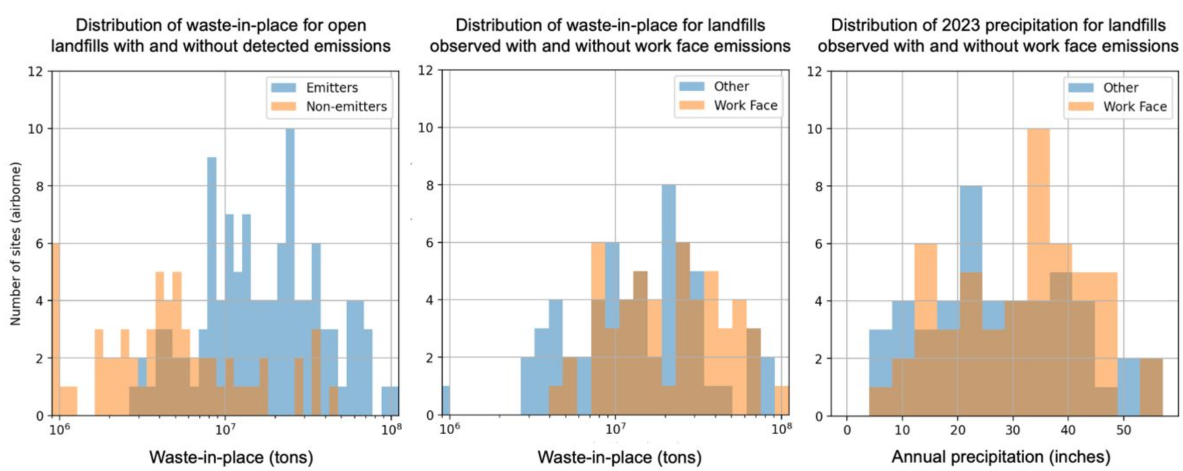

Figure S2. The distribution of landfill size and annual 2023 precipitation at the landfill. We show the distribution of landfill size (waste-in-place in short tons) for open landfills with and without observed point sources (left) and for emitting landfills with and without work face emissions (center). We also show the distribution of annual precipitation for 2023, as provided in the NOAA gridded precipitation product (4 km x 4 km; see text for citation), for emitting landfills with and without work face emissions (right). Note that the overlap of the distributions appears brown in color.

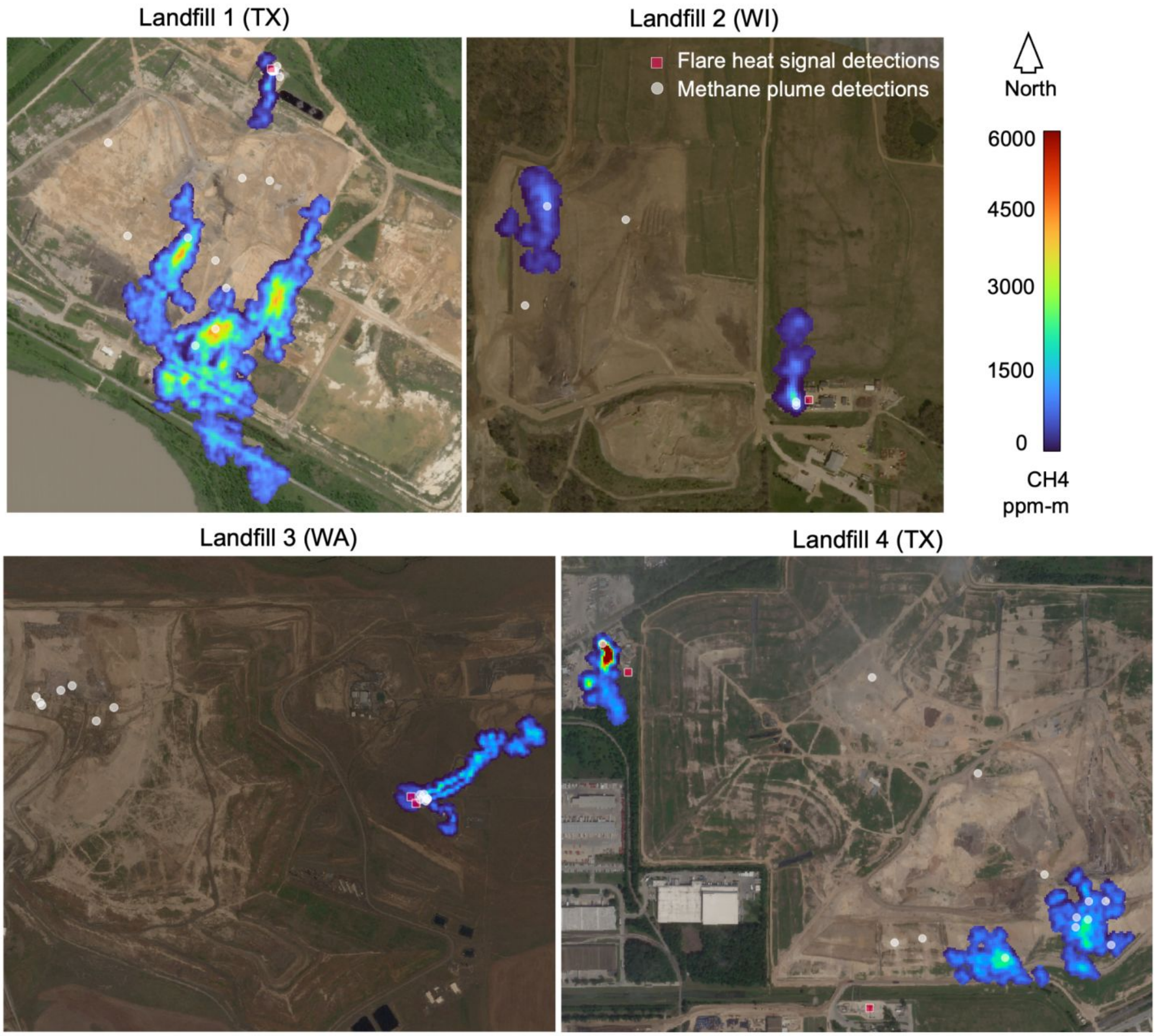

Figure S3. Landfill surface imagery, locations of methane sources and control stacks (e.g., flares), and methane plume images for Landfills 1-4 in Figure 4. For the 4 landfills, we show all methane plume origins (white circles) and all locations of detected heat signals from control stacks (red squares) from observations made in 2023. For each landfill, we show images of methane plumes from a select date (Landfill 1 - 4/16/2023; Landfill 2 - 5/11/2023; Landfill 3 - 7/22/2023; Landfill 4 - 4/16/2023). The landfill images are from the SkySat satellite and were captured within a few days of the methane observations. Landfill 3 has two side-by-side control stacks that showed the same behavior (i.e., emitting and active heat signal) throughout the period of observation. Landfill 4 has multiple control stacks: at the RNG facility to the northwest, at a second RNG facility south of the landfill scales, and at the landfill flare station to the south of the landfill.

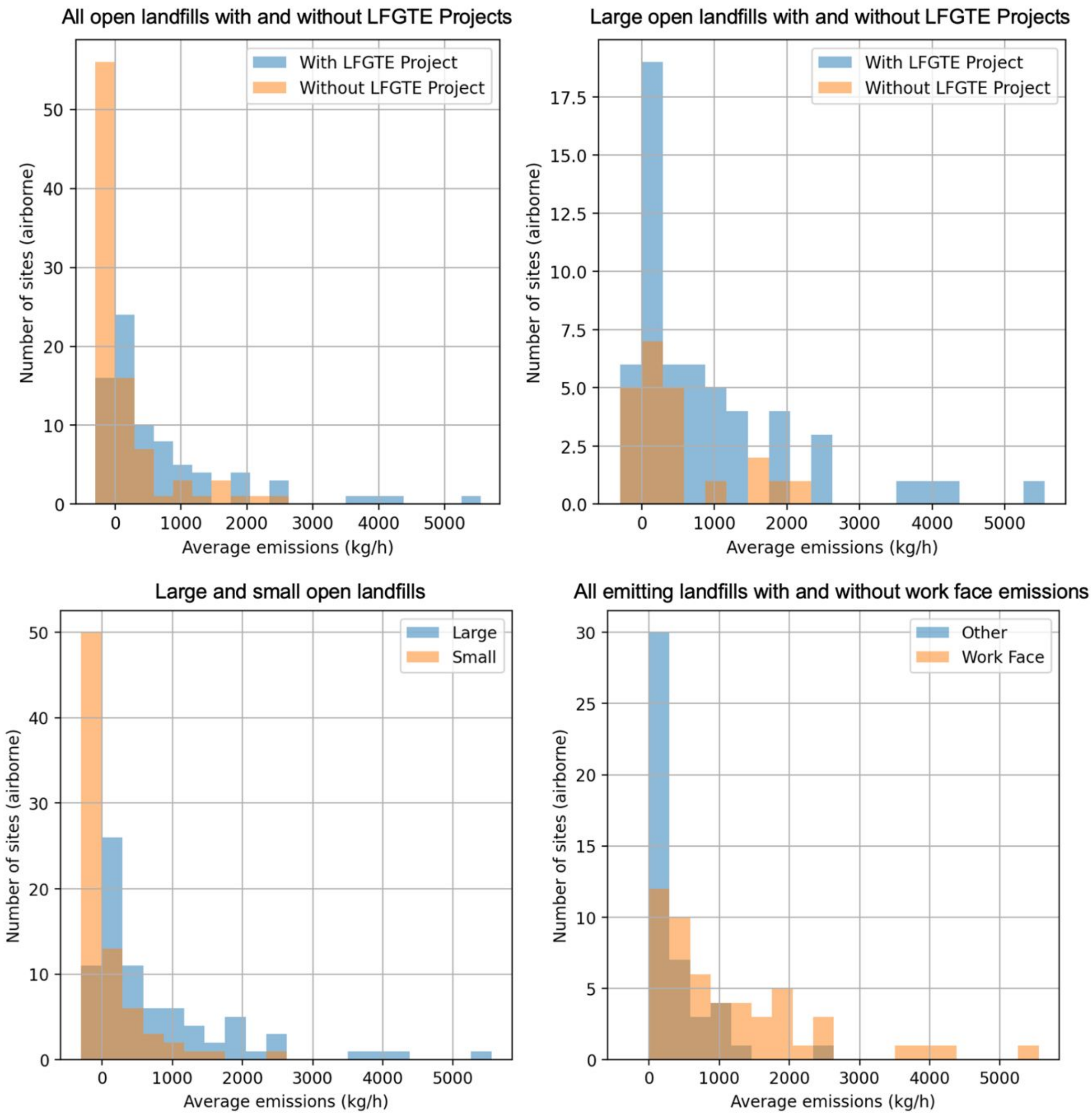

Figure S4. Distribution of average landfill methane emissions for landfills observed during airborne campaigns in 2023. In the top row, we show the distribution of average persistence adjusted emission rates for open landfills with and without landfill gas-to-energy (LFGTE) projects for all landfills observed (top left) and a subset of 'large' landfills (top right). Landfills were considered 'large' if their waste-in-place is greater than the median of open observed sites which was 9.8 million metric tons. The distribution of emissions is also shown for large versus small open landfills (bottom left) and for emitting landfills with and without work face emissions (bottom right). Landfill emission rates shown as below zero reflect those landfills with no observed point source emissions. The distributions shown do not include landfills that were observed to be emitting but have no published emission rates (see quality control methods described in the text). Note that the overlap of the distributions appears brown in color.

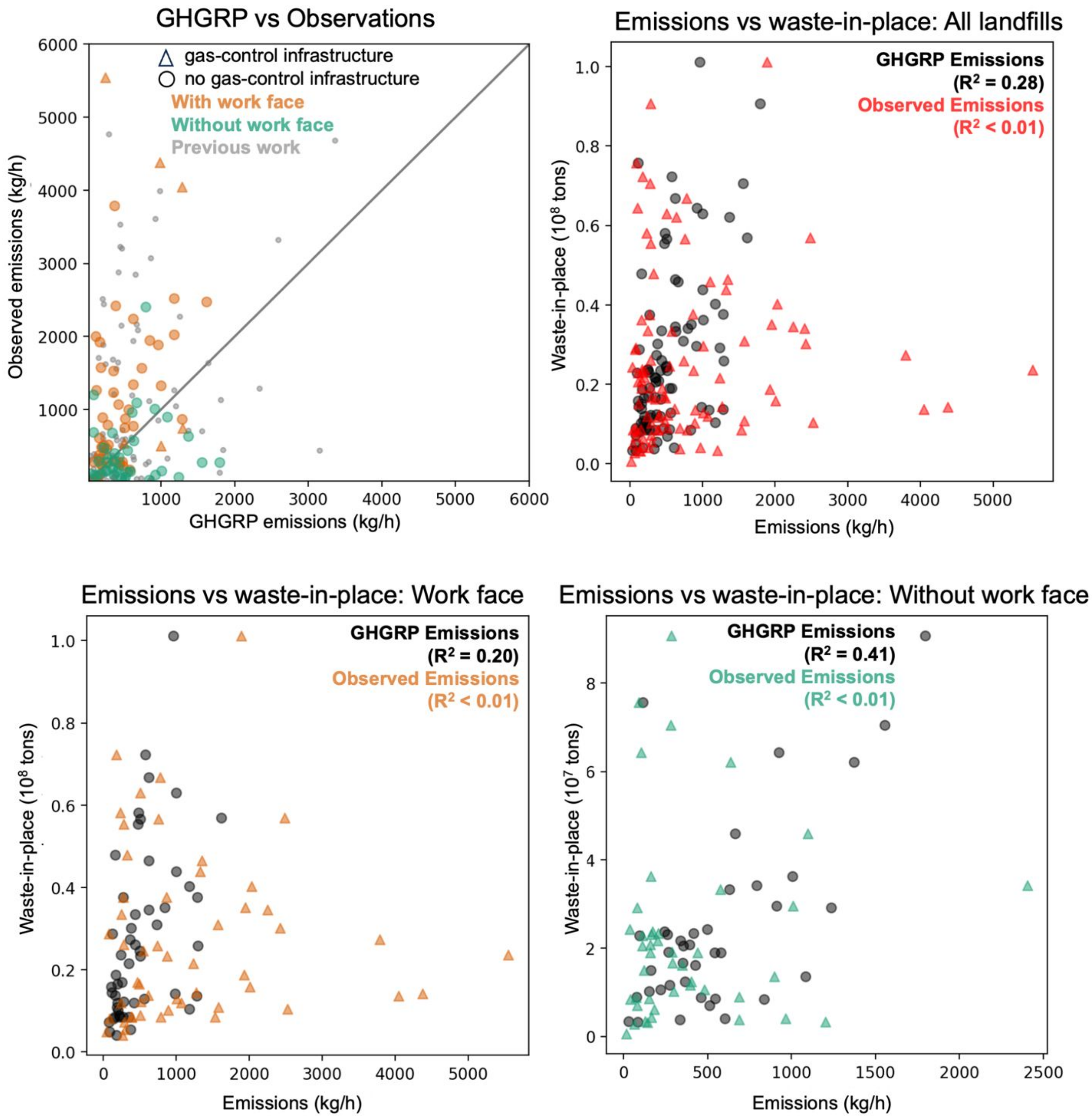

Figure S5. Observed landfill methane emissions compared to GHGRP reported emissions and compared to waste-in-place. For the top-left plot, estimated hourly emissions derived from the annual emissions reported to the GHGRP for 2022 are compared to observed emissions in 2023 separated by source type; we show landfills with evidence of work face emissions (orange) and landfills without evidence of work face emissions (green). Also for the top-left plot, landfills are separated by those with (triangle) and without (circle) at least 1 detected methane plume from gas-control infrastructure. Data from previous work, as described by Cusworth et al. (2024), are also shown for context but not separated by source type (gray). For the emissions vs waste-in-place comparisons (top right and bottom row plots), observed (triangles) and GHGRP estimated (black circles) emissions are shown compared to the mass of waste-in-place for each landfill. The bottom row shows this comparison for landfills with work face emissions (left; orange) and for landfills without work face emissions (right; green) as described above. The coefficient of determination (R^2) is also shown for the GHGRP and observed emissions in comparison to waste-in-place.

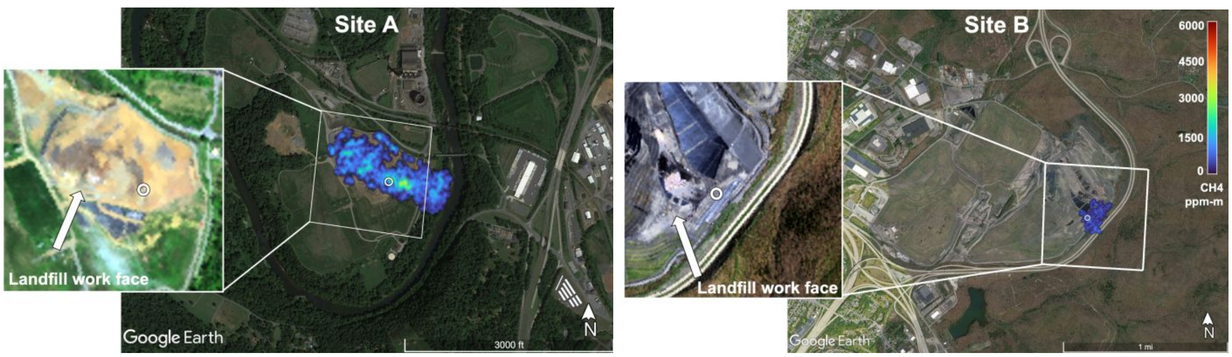

Figure S6. Methane plumes at Pennsylvania landfills observed in April 2021. Emissions for these landfills were attributed to the landfill work face. The images show observed methane plumes overlaid on a Google Earth Basemap (not contemporaneous with the observation). The inset images show the landfill surface observed by the instrument contemporaneously with the plume observations. The white ring shows the plume origin. The methane concentration color scale applies to both Site A and Site B.

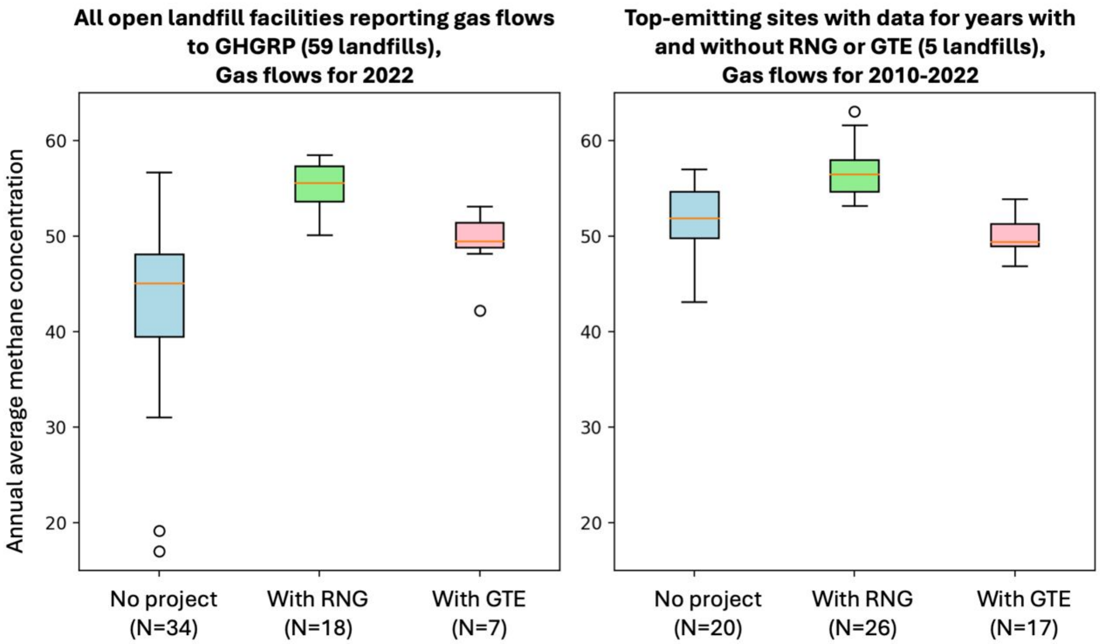

Figure S7. Methane concentrations (in percent methane) in landfill gas for Texas landfills reporting to the GHGRP. We separate landfills based on beneficial use project status according to LMOP (US EPA, 2023b), including those landfill facilities with no associated project (blue), renewable natural gas projects (RNG; green), and gas-to-electricity projects (GTE; pink). The left plot shows 2022 reported methane concentrations for all open, GHGRP reporting landfills in Texas. The right plot shows 2010-2022 reported methane concentrations for the top-emitting landfill facilities in Texas (persistence adjusted emission rates > 1500 kg/h) that report gas flow for years with and without RNG in 2010-2022. For each site and reporting year, we separately assess whether there was an operational GTE or RNG facility associated with the landfill for that year and assign the appropriate status. For the boxplot: the orange line shows the median value, the bottom and top of the colored boxes show the 25th and 75th percentile, respectively, and the black lines extending from the boxes show the minimum and maximum values with outliers shown as circles.

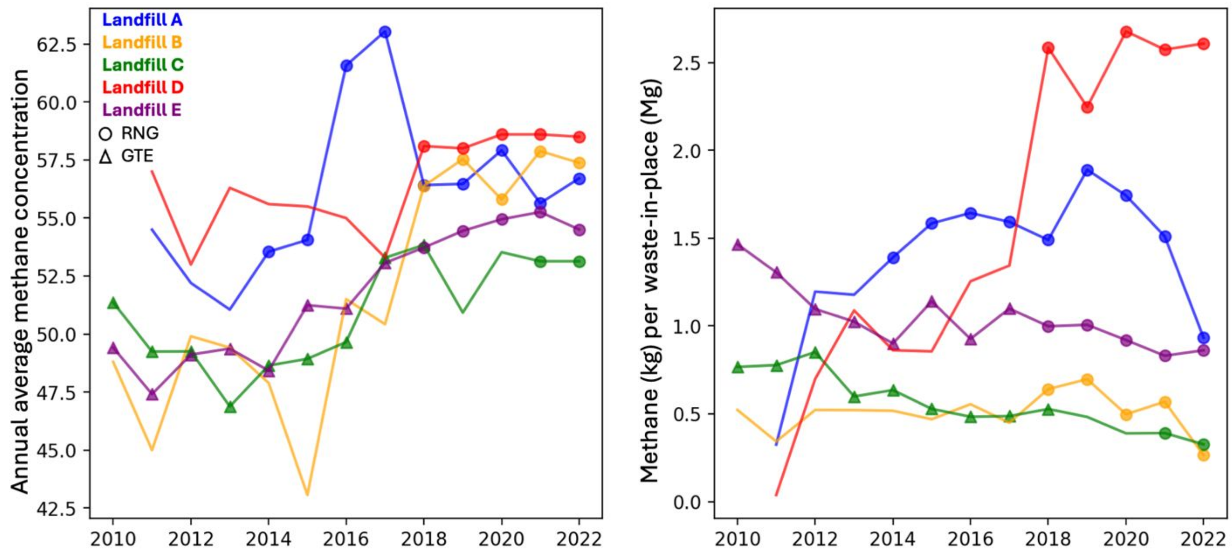

Figure S8. Methane concentrations in landfill gas (in percent methane; left) and methane collected per waste-in-place (right) for the top-emitting Texas landfills. We show Texas landfills that have 2023 observed emissions > 1500 kg/h and that report gas flow data for years with and without RNG in 2010-2022. Each landfill is shown as a unique color, labeled A-E, and the circles and triangles denote years with RNG and gas-to-electricity (GTE), respectively.